



## EFFECTS OF PRE-STRAIN HISTORY ON THE CYCLIC RESISTANCE OF OTTAWA F-65 SAND

A.M. Parra Bastidas <sup>(1)</sup>, R.W. Boulanger <sup>(2)</sup>, J.T. DeJong <sup>(3)</sup>, A.B. Price <sup>(4)</sup>

<sup>(1)</sup> Corresponding author and Ph. D. Candidate, Department of Civil and Environmental Engineering, University of California, Davis, CA, USA, [aparrabastidas@ucdavis.edu](mailto:aparrabastidas@ucdavis.edu)

<sup>(2)</sup> Professor, Department of Civil and Environmental Engineering, University of California, Davis, CA, USA, [rwboulanger@ucdavis.edu](mailto:rwboulanger@ucdavis.edu)

<sup>(3)</sup> Professor, Department of Civil and Environmental Engineering, University of California, Davis, CA, USA, [jdejong@ucdavis.edu](mailto:jdejong@ucdavis.edu)

<sup>(4)</sup> Ph. D. Candidate, Department of Civil and Environmental Engineering, University of California, Davis, CA, USA, [abprice@ucdavis.edu](mailto:abprice@ucdavis.edu)

### **Abstract**

The cyclic strength of a saturated sand can be expected to evolve in response to the cumulative effects of multiple earthquake events over geologic time. Prior laboratory studies have demonstrated that cyclic pre-straining can significantly increase or decrease the cyclic strength for future events, depending on the sand's properties and state variables (e.g., relative density, stress history), effective confining stresses, and dynamic strains (e.g., amplitudes and numbers of cycles). For example, prior studies have shown that small amplitude cyclic pre-straining tends to increase cyclic strength whereas large amplitude cyclic pre-straining can decrease cyclic strength for dense sand. The cumulative effect of repeated recurrent liquefaction and pre-straining events on the correlation between cyclic strength and void ratio have not, however, been examined. The present study examines the effects of repeated recurrent liquefaction and cyclic pre-straining on the cyclic strength of clean Ottawa F-65 sand. Cyclic direct simple shear tests are performed for a range of initial relative densities subjected to sequences of cyclic loading events. Each cyclic loading event consisted of uniform cyclic stress controlled loading to a maximum shear strain or maximum number of loading cycles, after which the specimen was allowed to reconsolidate prior to the next cyclic loading event. The evolution of cyclic loading behavior through these sequences of loading events are described. Recurrent liquefaction (i.e.,  $r_u = 100\%$  or  $\gamma_{\max} = 3\%$ ) and cyclic pre-straining without causing liquefaction caused significant increases in cyclic strength relative to virgin specimens across a range of loose to dense conditions, with the effects being greater for denser specimens. The observed responses and their implications for liquefaction triggering correlations in practice are discussed.

*Keywords: Pre-strain history, Cyclic strength, Liquefaction, Laboratory testing*



## 1. Introduction

Recurrent soil liquefaction has been observed at many sites during different earthquake events. Recent examples include the recurrence of liquefaction in natural deposits in the Christchurch, New Zealand area during the 2010-11 Canterbury Earthquake Sequence (Lees et al. [1]) and in artificial fills in the Tokyo area during the 2011 Tohoku earthquake (Wakamatsu [2]). Field studies have attempted to quantify the effects that liquefaction has on in-situ test results or a site's performance in subsequent earthquake events, but noticeable effects have been difficult to discern relative to the effects of spatial variability and other sources of uncertainty.

The repeated recurrence of liquefaction would be expected to produce a progressive evolution of soil properties throughout a soil profile. The schematic in Figure 1 illustrates how the accumulation of densification from repeated events would be expected to produce a state with greater resistance to liquefaction. The progression may be different at different depths in the soil profile, perhaps even with some loosening or weakening near the surface or beneath lower permeability layers that can impede upward water flow. Overall, however, the expectation would be that a sufficient number of strong shaking events would eventually improve the resistance of a site to liquefaction.

Laboratory element testing has shown that cyclic pre-straining can increase or decrease the cyclic strength of sand depending on a number of factors (Singh et al. [3], Goto et al. [4], Seed et al. [5], and Oda et al. [6]). For example, Seed et al. [5] conducted shaking table tests on air pluviated sand specimens, in which the specimens were first subjected to short-duration cyclic loading events (2½-3 cycles with reconsolidation between events) followed by long-duration cyclic loading. The short-duration cyclic loading (or pre-straining events) caused excess pore pressure ratios of 0.3 to 0.05 with little change in dry density during reconsolidation, but still caused an increase in cyclic strength (Fig. 2) and decrease in the rate of excess pore water pressure generation during the long-duration cyclic loading. Oda et al. [6] performed undrained cyclic triaxial tests on air pluviated, dense Toyoura sand specimens that had been reconsolidated after being cyclically loaded undrained to different levels of peak axial strain ( $\epsilon_{a,pre}$ ). They observed that the cyclic strength of these dense specimens was reduced when the value of  $\epsilon_{a,pre}$  was greater than 1% (Fig. 3); this was observed even when the prior cyclic loading and reconsolidation caused the relative density ( $D_R$ ) of the specimens to increase. They associated the reduction of liquefaction resistance with the development of specimen anisotropy, with sand particles envisioned to have formed column-like structures (even if the global void ratio did not change significantly) which were less stable when the specimen was stressed perpendicular to the elongation direction.

Centrifuge tests have also been used to study the effect of prior cyclic loading on the cyclic strength of sands. El-Sekelly et al. [7] subjected a centrifuge model of a level silty sand profile to 91 shaking events that included events with 5 cycles of loading with a maximum acceleration of about 0.035 g and events with 15 cycles of loading with a maximum acceleration of about 0.040 g and 0.12 g; events were followed by full pore water pressure dissipation. They concluded that pre-shaking with small acceleration events reduced the maximum excess pore pressure ratios and the depths at which liquefaction was triggered within the model; however, this effect was reset when the model was shaken with events with higher accelerations, and this resetting effect diminished towards the end of the experiments. Overall, pre-shaking increased the cyclic strength of a silty sand deposit over the progression of shaking events. El-Sekelly et al. [8] performed similar tests with clean Ottawa F#55 sand and obtained similar findings. Darby et al. [9] conducted a centrifuge test with multiple shaking events and inflight cone penetration resistance measurements in Ottawa F-65 sand. The model was subjected to sixteen shaking events of 15 cycles of sinusoidal acceleration followed by full pore pressure dissipation; the peak base acceleration was between 0.018 to 0.09 g. They concluded that the cumulative effect of these sixteen events, of which five triggered liquefaction, resulted in about a 160% increase in the average cone tip resistance from about 2.5 MPa to 6.5 MPa and an associated modest increase in cyclic strength.

The results of the above laboratory and centrifuge testing studies demonstrate that the effect of cyclic pre-straining on the cyclic strength of sands depends on: the amplitude and number of prior strain cycles; the initial  $D_R$  and the changes in  $D_R$  due to prior cyclic loading; the changes in fabric due to recurrent cyclic loading, with the changes depending on the amplitude of the cyclic strains; and any destruction of prior ageing, cementation, over-consolidation, or cyclic pre-straining effects if the most recent pre-strains are of large enough amplitude.

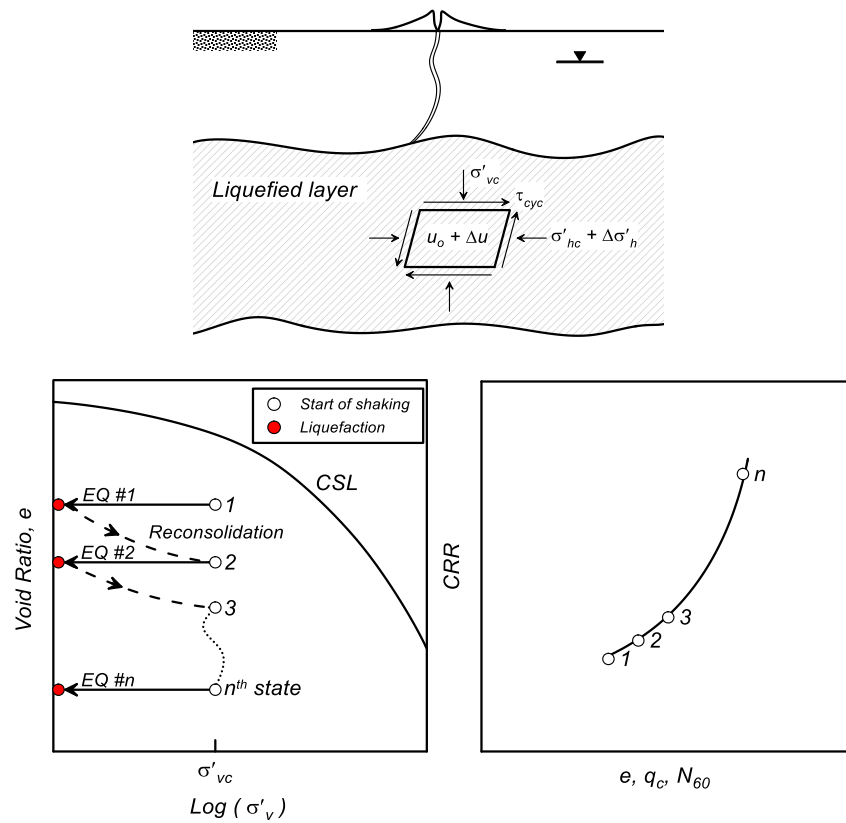


Fig. 1 - Conceptual effect of recurrent liquefaction events: (a) soil element in liquefied layer, (b) void ratio–vertical effective stress paths for a series of earthquake loadings causing liquefaction and subsequent reconsolidation, and (c) evolution of cyclic strength versus indices of density (after Price et al. [10])

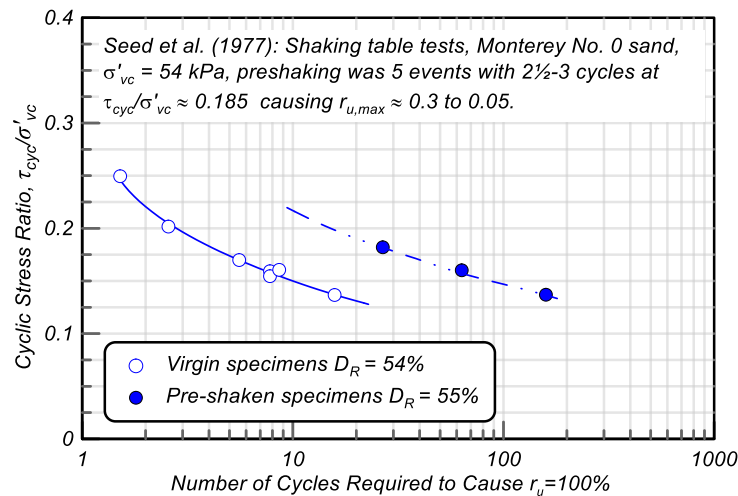


Fig. 2 - Cyclic stress ratio versus number of uniform load cycles to cause  $r_u = 100\%$  from shake table tests on air pluviated sand specimens with and without pre-straining (after Seed et al. [5])

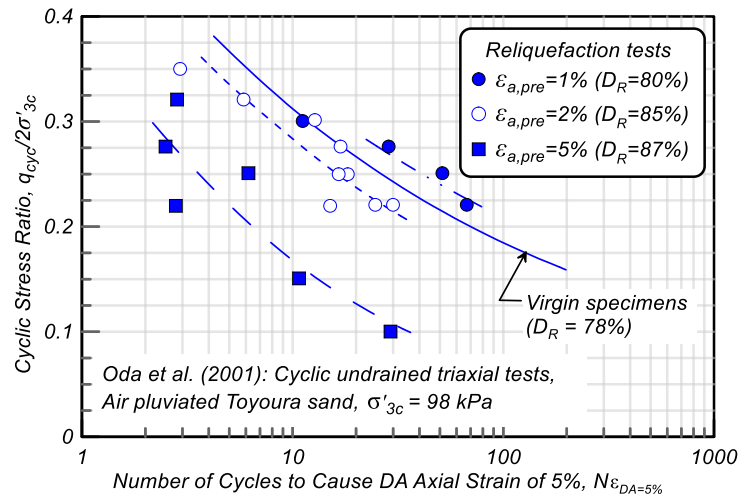


Fig. 3 - Cyclic stress ratio versus number of uniform load cycles to cause double amplitude (DA) axial strain of 5% from cyclic undrained triaxial tests results on air pluviated Toyoura sand specimens with pre-straining to different peak axial strains (after Oda et al. [6])

The purpose of this paper is to examine the effect of repeated recurrent liquefaction and cyclic pre-straining on the cyclic strength of clean Ottawa F-65 sand. The results serve two purposes. First, this sand is a standard reference sand used in centrifuge model studies, including at the Center for Geotechnical Modeling at the University of California at Davis. Centrifuge models are frequently subjected to multiple shaking events, such that the evolution of cyclic strengths with pre-straining is an issue that requires attention in the calibration of nonlinear numerical models. Second, the results provide further insights on the evolution of cyclic strengths with multiple pre-straining stages. This paper describes the characteristics of Ottawa F-65 sand, the experimental procedures used to conduct direct simple shear (DSS) tests with repeated loadings, results from monotonic and cyclic DSS tests on virgin specimens, results from cyclic pre-straining DSS tests, and discussion of the effects that cyclic pre-straining had on cyclic strengths and cyclic loading behaviors. Finally, some of the implications of the findings are discussed.

## 2. Experimental Approach

The effect of repeated recurrent liquefaction and cyclic pre-straining on the cyclic loading behavior of Ottawa F-65 sand was evaluated using DSS tests. The characteristics of the sand, the specimen preparation procedures, and the DSS testing procedures are described in this section. Additional test data are in Parra Bastidas et al. [11].

Ottawa F-65 sand is a quartzitic uniform sand with rounded grains produced by mining of fine-grained St. Peter sandstone deposits near Ottawa, Illinois. The silica content of this sand is 99.5% [12]. The coefficient of uniformity ( $C_u$ ) is 1.61, the coefficient of curvature ( $C_c$ ) is 0.96, the fines content is 0.17% and the specific gravity of solids ( $G_s$ ) is 2.65. The maximum dry density is  $1759 \text{ kg/m}^3$  by the Japanese Method JIS A 1224 (JIS [13]) standard method and the minimum dry density is  $1446 \text{ kg/m}^3$  by ASTM D4254-00 (ASTM [14]) standard method. The corresponding minimum and maximum void ratios are 0.507 and 0.833, respectively.

Specimens were prepared dry and were placed in a GEOTAC DSS apparatus for saturation, consolidation and shearing. Loose specimens were prepared by the dry funnel deposition (DFD) method and dense specimens were prepared by the air pluviation (AP) method. Specimens were subjected to a seating load of 10 kPa in the DSS apparatus. Specimens were saturated in the DSS apparatus with approximately 100 ml of de-ionized water which flowed by gravity. Specimens were consolidated using load increment ratios of about 2.0 until the final consolidation stress was reached. Each intermediate load increment was applied for 5 minutes, whereas the final load was maintained for one hour to allow the specimen to consolidate and creep before shearing.

Undrained simple shear tests were performed under a constant height condition that is equivalent to an undrained shearing condition on the DSS apparatus (Dyvik et al. [15]). Monotonic tests on virgin specimens were performed at a shear strain rate of 50% per hour and to a maximum shear strain ( $\gamma_{max}$ ) of approximately 15%. Cyclic tests on virgin specimens were performed at a shear strain rate of 50% per hour, but with a stress criterion for reversal of loading directions to produce uniform cyclic stress ratio loadings. Cyclic loading was continued to a  $\gamma_{max}$  of approximately 5% in all tests of virgin specimens.

The loading procedures for pre-strained specimens is similar to the process followed by Price et al. [10]. Each cyclic loading stage consisted of uniform cyclic stress ratio loading until a  $\gamma_{max}$  of approximately 3% or a maximum of 100 loading cycles was reached. The specimen was then re-centered to the position of absolute zero shear strain, the constant-height restraints were released, and the specimen was reconsolidated using the same procedures used for virgin consolidation. This process was followed for all cyclic loading stages. The cyclic stress ratio for the cyclic loading stages was increased in a sequence of steps, with several cyclic loading stages being performed at each step. At each value of cyclic stress ratio, cyclic loading stages were repeated until the specimen resisted 100 cycles of loading without reaching  $\gamma_{max} = 3\%$ . The cyclic stress ratio was then increased for the next series of cyclic loading stages. The cyclic stress ratios applied to the loose specimens were 0.12, 0.18, 0.25, 0.40 and 0.80. The cyclic stress ratios applied to the dense specimens were 0.25, 0.40 and 0.80.

### 3. Monotonic and Cyclic DSS Results for Virgin Specimens

Monotonic undrained DSS responses for loose and dense normally consolidated (NC) virgin specimens consolidated to a vertical effective consolidation stress ( $\sigma'_{vc}$ ) of a 100 kPa are shown in Fig. 4. Dilative tendencies increase with relative density ( $D_R$ ). The specimen with a  $D_R = 15\%$  shows little change in shear stress and vertical effective stress after a shear strain ( $\gamma$ ) of approximately 2%, indicating this specimen is approximately at a critical state condition. The specimen with a  $D_R = 30\%$  shows an initial contractive tendency, followed by a quasi-steady state behavior at a  $\gamma$  of approximately 3 to 5%, followed by a dilatant tendency after  $\gamma$  of approximately 5%. The specimen with a  $D_R = 78\%$  shows a smaller initial contractive tendency followed by a strong dilatant tendency with no quasi-steady behavior.

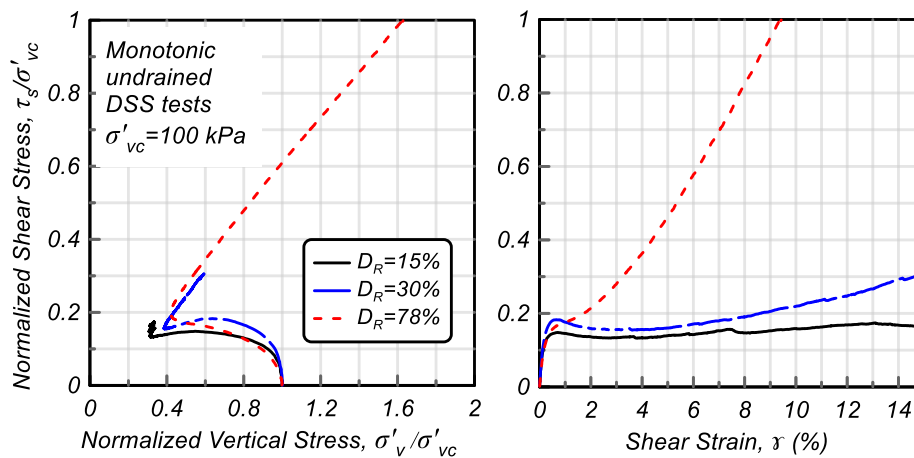


Fig. 4 - Monotonic responses for loose and dense virgin specimens of Ottawa sand F-65

The cyclic resistance ratio (CRR) is plotted vs. the number of loading cycles ( $N$ ) to  $\gamma_{max} = 3\%$  for loose and dense NC virgin specimens consolidated to  $\sigma'_{vc} = 100$  kPa in Fig. 5. The loose specimens had a  $D_R$  of about 40% and the dense specimens a  $D_R$  of about 80%. The CRR to cause  $\gamma_{max} = 3\%$  in a certain number of cycles increases with  $D_R$ . The CRR versus  $N$  curves were each fit with a power law and the exponent  $b$  (which defines the negative slope of the curve) was determined to be 0.15 for the loose specimens and 0.17 for the dense specimens.

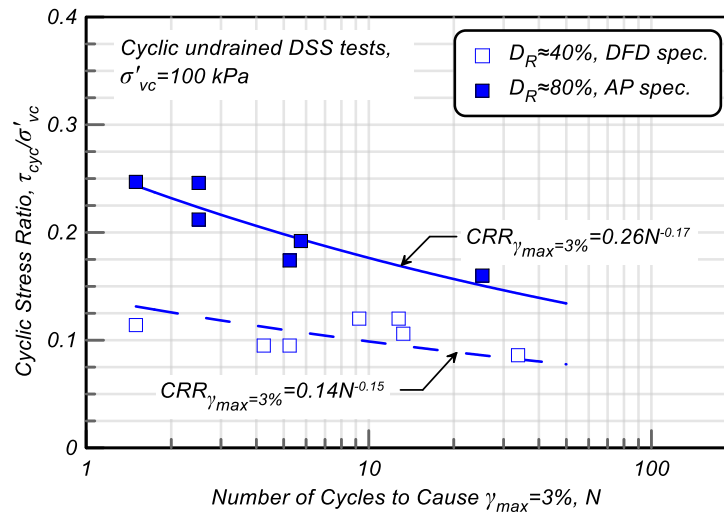


Fig. 5 - Cyclic resistance curves for loose and dense specimens of Ottawa sand F-65

#### 4. Cyclic DSS with pre-straining

Undrained cyclic DSS with pre-straining tests were conducted on loose and dense NC specimens consolidated to  $\sigma'_{vc} = 100$  kPa. An example loading sequence is illustrated in Fig. 6 for test PS6, showing the CSR that was applied during each cyclic shearing stage, the corresponding the number of cycles to  $\gamma_{max}=3\%$  and the  $D_R$  of the specimen at the start of each loading. This specimen was subjected to 9 stages of cyclic loading and reconsolidation with CSR = 0.12 (stages A1 to A9), 1 stage of cyclic loading and reconsolidation with CSR = 0.18 (stage B1), 1 stage of cyclic loading and reconsolidation with CSR = 0.25 (stage C1), 2 stages of cyclic loading and reconsolidation with CSR = 0.40 (stage D1 to D2) and 3 stages of cyclic loading and reconsolidation with CSR 0.80 (stages E1 to E3). The  $D_R$  progressively increased throughout the sequence from its initial value of 25% to its final value of 83%. The number of cycles required to reach  $\gamma_{max} = 3\%$  increased in each loading stage with the same CSR. Note that  $\gamma_{max}$  did not reach 3% in the loading stages that stopped at 100 cycles (stages A9, B1, C1, D2, and E3).

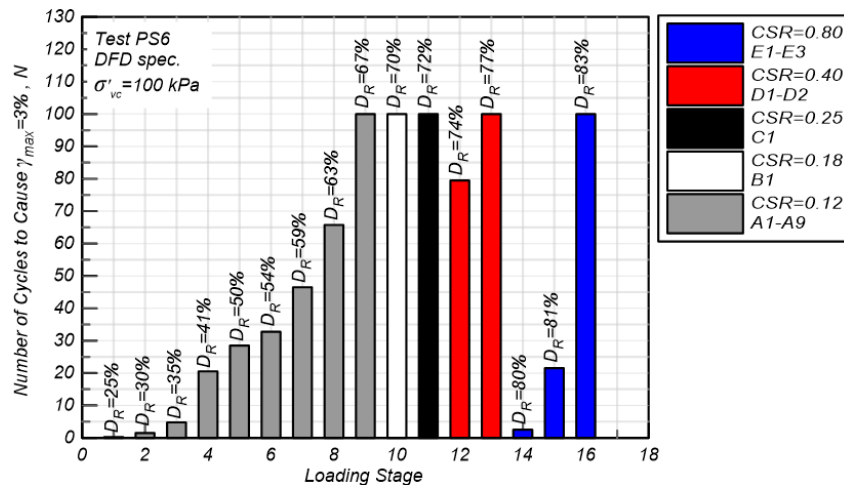


Fig. 6 - Number of cycles to peak 3% shear strain vs. loading stage on test PS6

The cyclic loading responses of test PS6 for select cyclic loading stages are shown Fig. 7; this figure shows normalized shear stress versus shear strain (top row), stress paths (middle row) and normalized vertical effective stress versus shear strain (bottom row) for the cyclic loading stages A3 (1<sup>st</sup> column), A6 (2<sup>nd</sup> column), B1 (3<sup>rd</sup> column) and D1 (4<sup>th</sup> column) (Fig. 8). The specimen exhibited increased dilative tendencies as the specimen became denser with each loading stage. The rate of shear strain accumulation after strains exceeded about 1% became progressively smaller with each loading stage at the same CSR and sometimes smaller even when the CSR was increased to the next level.

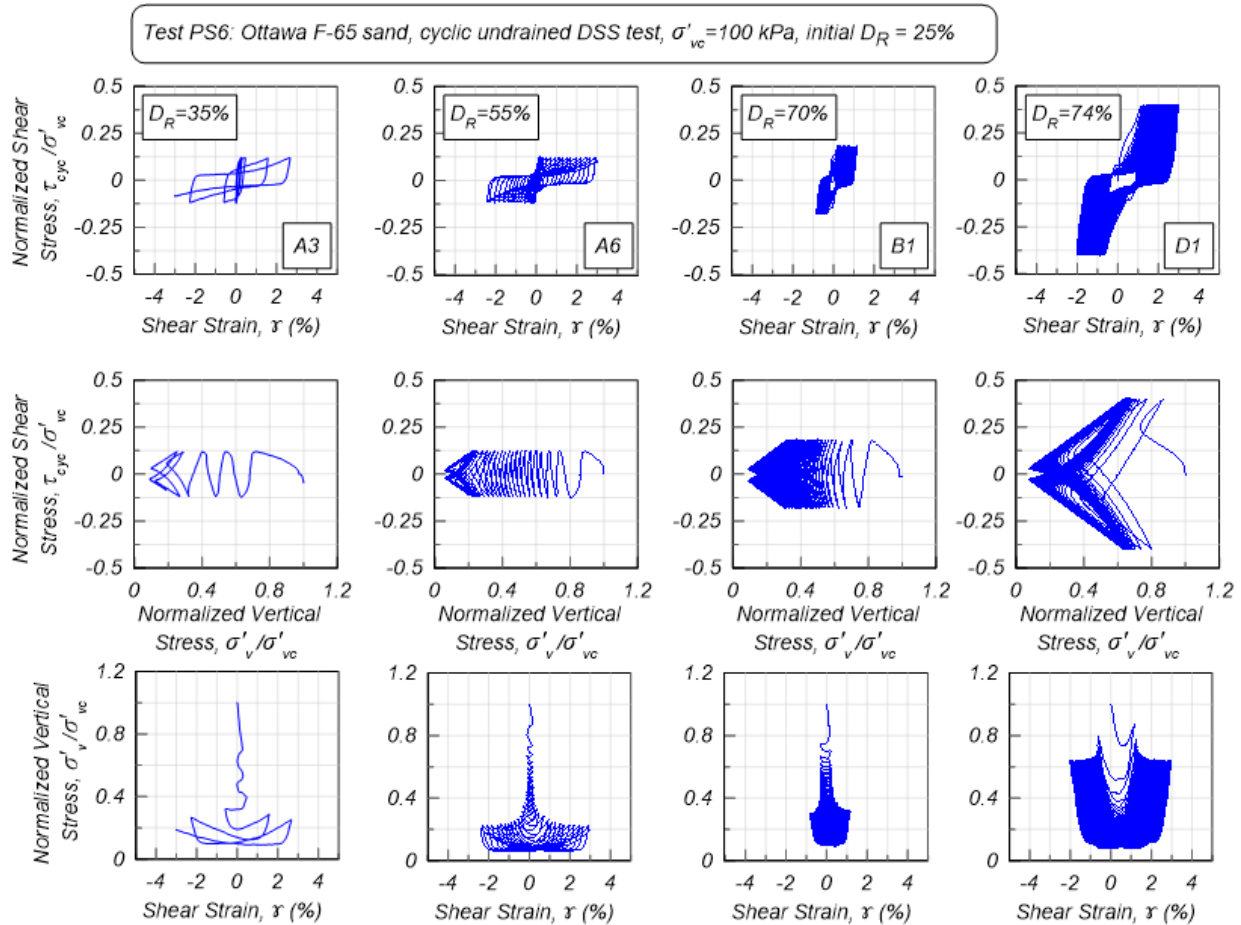


Fig. 7 - Undrained cyclic DSS test results from loading stages A3, A6, B1 and D1 for test PS6

The behaviors evident in Figs. 6 and 7 are representative of those observed in other tests on NC specimens independent of their initial  $D_R$ . Specimens that began with a higher initial  $D_R$  took fewer loading stages to develop a given level of cyclic strength, but the cyclic loading behavior at any one stage was dependent on the prior loading history as well as the current value of  $D_R$ , as illustrated below.

The cyclic loading responses of a virgin specimen and a pre-strained specimen at similar  $D_R$  are presented in Fig. 8; the response the virgin specimen from test V23 with initial  $D_R = 77\%$  is plotted in Fig. 8a and the response of the pre-strained specimen from test PS6 in the loading stage D1 with a current  $D_R = 74\%$  is plotted in Fig. 8b. The pre-strained specimen had stronger dilative tendencies than the virgin specimen, even though the virgin specimen has a slightly higher initial  $D_R$ . The pre-strained specimen had a slower accumulation of shear strain per loading cycle after strains exceed about 1%. However, the pre-strained specimen accumulated approximately 1% shear strain during the first quarter of the first loading cycle whereas the virgin specimen accumulated only 0.5% shear strain during the first quarter of the first loading cycle. Thus, the pre-strained

specimen reached 1% strain more quickly than the virgin specimen, but then accumulated strains slower than the virgin specimen subsequently. The net effect was that the pre-strained specimen had a greater resistance to developing a maximum shear strain of 3% than the virgin specimen. The pre-strained specimen had a lower phase transformation angle ( $\approx 20^\circ$ ) during the first quarter cycle of loading than the virgin specimen during its second loading cycle ( $\approx 26^\circ$ ) or the virgin specimen from the monotonic test ( $\approx 29^\circ$  on Fig. 4). The lower transformation angle in the pre-strained specimen might be due to the more stable fabric that developed across the shearing stages, even though this specimen was prepared initially looser than the virgin specimen. The difference in the specimen's preparation methods might also have had some influence in the difference in the phase transformation angles mobilized by the virgin and the pre-strained specimens.

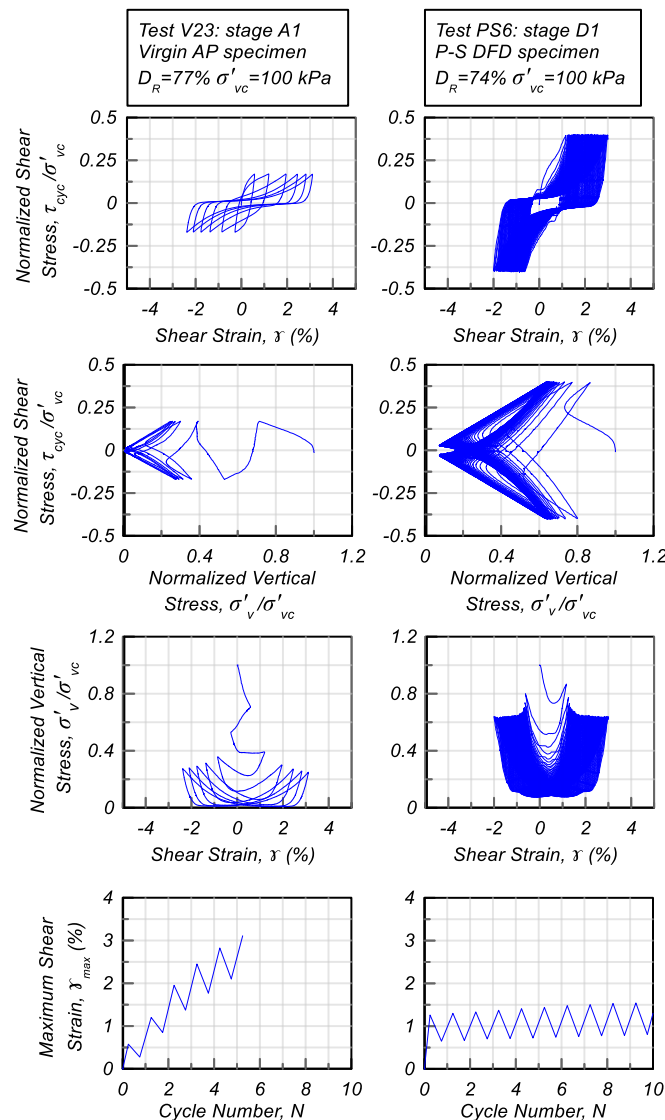


Fig. 8 - Undrained cyclic DSS test results on dense initially NC specimens: (a) virgin specimen from test V23, and (b) pre-strained specimen from test PS6 during loading stage D1

The evolution of the CRR with each loading stage on pre-strained specimens was evaluated by estimating the CRR for  $\gamma_{max} = 1\%$  or  $3\%$  in 15 cycles for each loading stage. The  $CSR_{N=15}$  were obtained from converting the applied CSRs to equivalent  $CSR_{N=15}$  using the process described by Idriss and Boulanger [16]. For those loading stages that did not reach  $\gamma_{max} = 3\%$  before the test was stopped at 100 cycles, the equivalent  $CSR_{N=15}$

represents a lower bound estimate for the  $CRR_{N=15}$  against  $\gamma_{max} = 3\%$ . The above process applied to the pre-strained specimen in test PS6 and a failure criterion of  $\gamma_{max} = 3\%$  is shown in Fig. 9. The parameter  $b$ , which is the slope of the  $\log(CRR)$  versus  $\log(N)$  curves, was taken as 0.15 for both virgin and pre-strained specimens with  $D_R < 60\%$  and 0.17 for all denser specimens. The parameter  $b$  was assumed to be equal for virgin and pre-strained specimens and for either failure criterion, although the potential evolution of  $b$  with cyclic pre-straining and its dependence on the failure criterion warrant further investigation.

The  $CRR_{N=15}$  for  $\gamma_{max} = 1\%$  or  $3\%$  from test PS6 are plotted versus the average (global) void ratio ( $e$ ) for each cyclic loading stage in Fig. 10. The  $CRR_{N=15}$  to  $\gamma_{max} = 1\%$  and  $3\%$  were about the same when the specimen was loose (i.e.,  $e > 0.65$ ). The  $CRR_{N=15}$  for  $\gamma_{max} = 3\%$  then became progressively greater than for  $\gamma_{max} = 1\%$  as the void ratio progressively decreased to smaller values. At these lower void ratios, high  $r_u$  values and  $\gamma_{max} = 1\%$  could generate fairly quickly, but the specimens were highly resistant to accumulating larger strains as evident in the stress-strain responses shown previously in Fig. 7 and 8. The  $CRR_{N=15}$  for  $\gamma_{max} = 3\%$  became greater than unity when the average void ratio had decreased to about 0.56, corresponding to an average (global)  $D_R$  of about 83%.

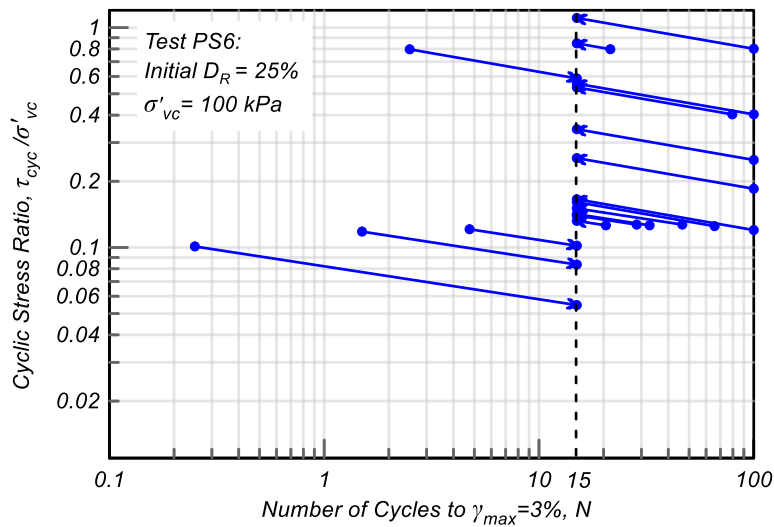


Fig. 9 - Conversion of applied CSR to  $CSR_{N=15}$  cycles for  $\gamma_{max} = 3\%$  for each loading stage in test PS6

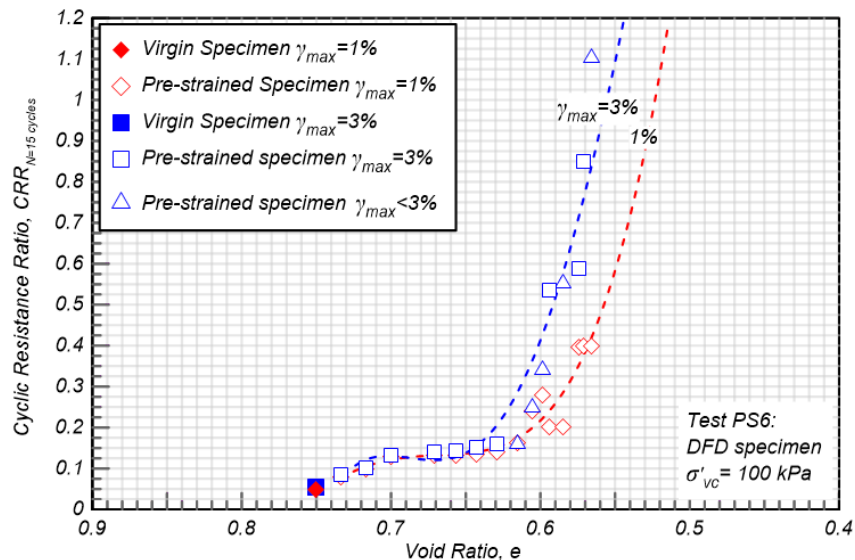


Fig. 10 - Evolution of the  $CRR_{N=15}$  for  $\gamma_{max}$  of 1% and 3% versus average void ratio for test PS6

The  $CRR_{N=15}$  to  $\gamma_{max} = 3\%$  for virgin specimens in tests V4, V7, V19, V23, V25 and V62 and pre-strained specimens in tests PS3, PS6, PS10, PS11 and PS12 are plotted together versus average (global) void ratio in Fig. 11. Loose virgin specimens ( $0.68 < e < 0.73$ ) had about 10-50% lower  $CRR_{N=15}$  values than pre-strained specimens over the same void ratio range. Dense virgin specimens ( $0.56 < e < 0.58$ ) had 40-55% lower  $CRR_{N=15}$  values than pre-strained specimens over the same void ratio range. The greater effect of pre-straining on the denser specimens could be partly due to the different sample preparation methods used to prepare the initially loose (dry funnel deposition) and dense (dry air pluviation) specimens. The cyclic strengths for virgin specimens would be expected to depend on preparation method (e.g., Mulilis et al. [17]), whereas the cyclic strengths for specimens after several cyclic loading stages would likely be less dependent on the preparation method. Nonetheless, it appears that pre-straining had a stronger effect on the rate of shear strain accumulation after  $r_u \approx 1.0$  developed, regardless of initial placement method (e.g., Figs. 7 and 8).

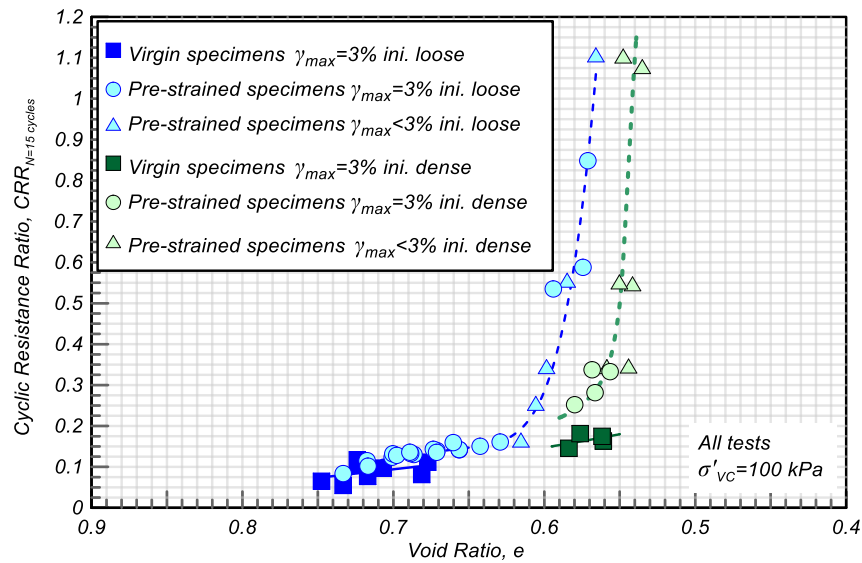


Fig. 11 - Evolution of the  $CRR_{N=15}$  to  $\gamma_{max} = 3\%$  versus average void ratio for virgin and pre-strain specimens

## 5. Discussion

The repetition of multiple cyclic loading stages on single DSS specimens are likely to have produced non-uniform distributions of void ratio throughout the specimens. For example, Gilbert [18] measured void ratio non-uniformities in triaxial specimens after a single stage of undrained cyclic loading to large axial strains. None of the specimens tested herein developed visible offsets in the stacked confining rings, which suggests that strong shear localizations did not develop in these tests. Nonetheless, it is reasonable to assume that certain zones in the DSS specimens will be denser and others looser than represented by the average, or global, void ratio. Evaluating these non-uniformities and their effects on specimen behavior would benefit from quantitative measurements of local void ratios using techniques like those used by Frost and Jang [19].

Evaluating the effect of pre-straining on liquefaction triggering correlations in sands will require parallel examination of how pre-straining affects both cyclic strengths and the results of in-situ test measurements. A promising approach to evaluate this issue is the use of centrifuge and shaking table tests, such as recently explored by El-Sekelly et al. [8] and Darby et al. [9]. These studies are expected to provide improved understanding of how recurrent liquefaction triggering affects liquefaction resistance and our ability to evaluate liquefaction resistance in young, uncemented sands.



The effect of multiple earthquake events on a site's liquefaction resistance over geologic time will be further complicated by other mechanisms, including ageing, cementation, and stress history (e.g., over-consolidation). In this regard, individual earthquake events could decrease a site's liquefaction resistance by destroying any benefits from ageing, cementation, or over-consolidation since the prior event. For example, Price et al. [in preparation] performed direct simple shear tests with multiple cyclic loading stages on initially over-consolidated non-plastic silt specimens, and showed that the cyclic strength of the over-consolidated specimens decreased after the first cyclic loading stage had triggered liquefaction. They further found that repeated recurrent liquefaction and reconsolidation stages eventually produced large net increases in cyclic strength. Thus, it appears reasonable to expect that the cumulative effect of multiple earthquake events would contribute, in general, to a progressive increase in a site's resistance to liquefaction-induced deformations over geologic time.

## 6. Conclusions

The cumulative effects of repeated recurrent liquefaction and cyclic pre-straining on the cyclic strength of clean Ottawa F-65 sand was evaluated using cyclic direct simple shear tests with multiple stages of uniform cyclic loading followed by reconsolidation. For example, the cyclic resistance ratio against a peak shear strain of 3% in 15 uniform loading cycles was increased from about 0.06 for a virgin loose specimen (initial relative density of 25%) to greater than 0.6 after a sequence of 14 cyclic loading stages (9 of which triggered liquefaction) had increased the specimen's relative density to about 80%.

Recurrent liquefaction and cyclic pre-straining caused significant increases in cyclic strength relative to virgin specimens across a range of loose to dense initial conditions, with the effects being stronger for denser specimens. The pre-straining history was particularly effective at reducing the rate of shear strain accumulation during uniform cyclic loading after  $r_v \approx 1.0$  developed (or after shear strains exceeded about 0.5-1.0%). The beneficial effects of recurrent liquefaction and cyclic pre-straining are attributed to a combination of densification and the evolution of a more stable fabric within the test specimens.

The results of the present study provide a basis for evaluating how the cyclic loading behavior of Ottawa F-65 sand may evolve in centrifuge or shaking table model tests subjected to multiple shaking events. The results also provide insights on the role that progressive densification and pre-straining may play in natural deposits subject to multiple earthquake events, although in-situ behaviors over geologic time will also be affected by other mechanisms such as ageing, cementation, and stress history (e.g., over-consolidation).

## 7. Acknowledgements

This project has been supported by COLCIENCIAS call 529 of 2011 doctoral loan-scholarship program. Any opinions, findings, or conclusions expressed herein are those of the authors and do not reflect the views of this organization.

## 8. References

- [1] Lees J J, Ballagh R H, Orense R P, van Ballegooy S (2015): CPT-based analysis of liquefaction and re-liquefaction following the Canterbury earthquake sequence. *Soil Dynamics and Earthquake Engineering*, **79**, 304-314.
- [2] Wakamatsu, K (2012): Recurrent liquefaction induced by the 2011 Great East Japan earthquake compared with the 1987 earthquake. *The International Symposium on Engineering Lessons Learned from the 2011 Great East Japan Earthquake*, Tokyo, Japan.
- [3] Singh S, Seed H B, Chan C K (1982): Undisturbed sampling of saturated sands by freezing. *Journal of the Geotechnical Engineering Division ASCE*, **108** (2), 247-64.
- [4] Goto S, Nishio S (1988): Influence of freeze thaw history on undrained cyclic strength of sandy soils (in Japanese). *Symposium on Undrained Cyclic Tests on Soils*, Japan.



- [5] Seed B, Mori K, Clarence K, Chan M (1977): Influence of seismic history on liquefaction of sands. *Journal of the Geotechnical Engineering Division ASCE*, **103** (4), 257-270.
- [6] Oda, M, Kawamoto K, Suzuki K, Fujimori H, Sato M (2001): Microstructural interpretation on reliquefaction of saturated granular soils under cyclic loading. *Journal of Geotechnical and Geoenvironmental Engineering ASCE*, **127** (5), 416-423.
- [7] El-Sekelly W, Abdoun T, Dobry R (2015): Liquefaction resistance of a silty sand deposit subjected to preshaking followed by extensive liquefaction. *Journal of Geotechnical and Geoenvironmental Engineering ASCE*, **142** (4), 04015101.
- [8] El-Sekelly W, Abdoun T, Dobry R (2016): PRESHAKE: a database for centrifuge modeling of the effect of seismic preshaking history on the liquefaction resistance of sands. *Earthquake Spectra* In-Press. doi: <http://dx.doi.org/10.1193/082515EQS131DP>
- [9] Darby K M, J D Bronner, Parra Bastidas A M, Boulanger R W, DeJong J T (2016): Effect of shaking history on cone penetration resistance and cyclic strength of saturated sand. *Geotechnical and Structural Engineering Congress*, Phoenix, AZ, USA.
- [10] Price A B, DeJong J T, Boulanger R W, Parra Bastidas A M, Moug D (2016): Effect of prior strain history on cyclic strength and CPT penetration resistance of silica silt. *Geotechnical and Structural Engineering Congress*. Phoenix, AZ, USA.
- [11] Parra Bastidas, A. M., Boulanger, R. W., Carey, T. J., and DeJong, J. T. (2016). "Ottawa F-65 Sand Data from Ana Maria Parra Bastidas," NEEShub, <http://dx.doi.org/10.17603/DS2MW2R>
- [12] US Silica (2016): <http://www.ussilica.com/products/ground-silica>, May 2, 2016.
- [13] JIS Committee (2009): *Test method for minimum and maximum densities of sands*. JIS A 1224.
- [14] ASTM (2000): *Standard test methods for minimum index density and unit weight of soils and calculation of relative density*. ASTM. D 4254 – 00.
- [15] Dyvik R, Berre T, Lacasse S, Raadim B (1987): Comparison of truly undrained and constant volume direct simple shear tests. *Geotechnique*, **37** (1), 3-10.
- [16] Idriss I M and Boulanger R W (2008): *Soil liquefaction during earthquakes*. EERI, MNO-12.
- [17] Mulilis J P, Seed H B, Chan C K, Mitchell J K, Arulanandan K (1977): Effect of sample preparation on sand liquefaction. *Journal of the Geotechnical Engineering Division ASCE*, **103** (2), 91-108.
- [18] Gilbert P A (1984): Investigation of density variation in triaxial test specimens of cohesionless soil subjected to cyclic and monotonic loading. Technical Report No. GL-84-10, U.S. Army Corps of Engineers, Waterways Experiment Station, Vicksburg, MS, USA.
- [19] Frost J D, Jang, D J (2000): Evolution of sand microstructure during shear. *Journal of Geotechnical and Geoenvironmental Engineering ASCE*, **126** (2), 116-30.